J Nanopart Res (2020) 22: 317
https://doi.org/10.1007/s11051-020-05050-y

RESEARCH PAPER

Effect of silica nanoparticles on mechanical properties of self-cured acrylic resin

C. M. B. Mussatto · E. M. N. Oliveira · K. Subramani · R. M. Papaléo · E. G. Mota

Received: 13 July 2020 / Accepted: 12 October 2020 / Published online: 21 October 2020

Abstract The purpose of this in vitro study is to evaluate the effect of the incorporation of silanized and non-silanized silica nanoparticles (~ 160 nm) in mechanical properties and surface roughness of self-cured acrylic resins. Five groups of samples were produced (with six specimens each), following the ISO 20795-1:2013 specifications. In the control group (Ctrl), no particles were added in the resin composition. Non-silanized silica nanoparticles were added either into the polymer (0.7 wt%, group G1) or into the monomer (0.27 wt%, G2). Two equivalent groups were formed for composite resins with silanized nanoparticles (groups G3 with 0.7 wt% incorporated into the polymer and G4 with 0.27 wt% added into the monomer). Data were submitted to Shapiro-Wilk ($\alpha = 0.05$) and ANOVA/Tukey ($\alpha = 0.05$). Nanoparticle-loaded resins showed similar microhardness as the control and a reduced flexural strength (20–27%) which was neither dependent on the amount of filler added nor in the method of nanoparticle incorporation. Surface silanization caused no major improvement in the mechanical behavior of the nanoresins but appears to improve dispersibility, as indicated by a smaller surface roughness.

Keywords PMMA · Dental composites · Nanoparticles · Silica

C. M. B. Mussatto (✉) · E. G. Mota
Department of Dentistry, School of Health Sciences, Pontifical Catholic University of Rio Grande do Sul (PUCRS), Porto Alegre, RS, Brazil
e-mail: cristiane.mussatto@edu.pucrs.br

E. M. N. Oliveira · R. M. Papaléo
Interdisciplinary Center of Nanoscience and Micro-Nanotechnology, School of Technology, Pontifical Catholic University of Rio Grande do Sul (PUCRS), RSPorto Alegre, Brazil

K. Subramani
Department of Advanced Education in Orthodontics and Dentofacial Orthopedics, College of Dental Medicine, Roseman University of Health Sciences, Henderson, NV, USA

Introduction

Self-curing acrylic resins used for manufacturing of dental prosthetics and temporary crowns remain in the mouth of patients, usually for long periods of time, serving, for example, as pulp and periodontal protection during the whole treatment (Kim and Watts 2004a). Therefore, it is very important for such dental materials to have adequate mechanical properties, including resistance to fracture; high flexural strength, typically larger than 60 MPa (ISO 20795-1 2013); and sufficient hardness (Da Silva et al. 2012; Balos et al. 2014; Cevik and Bicer 2016). In addition, surface roughness levels between 0.15 and 0.30 μm are desirable in order to diminish oral microbiota retention and maintain the health of periodontal tissues and patient comfort (Yamauchi et al. 1990; Bollen et al. 1997; Borchers et al. 1999).

Studies to improve the mechanical behavior of acrylic resins have started with thermopolymerizable resins reinforced with pre- and post-polymerized glass fibers, used in dental prosthetics (Karacaer et al. 2003; Kanie et al. 2004; Kim and Watts 2004b; Bertassoni et al.

2008). In these studies, a significant increase in flexural strength, elastic modulus, and impact resistance of the reinforced denture bases has been found. Subsequently, other materials with various shapes and sizes such as glass flakes (Franklin et al. 2005), polytetrafluoroethylene (Straioto et al. 2010), prepolymers (Cevik and Bicer 2016), and carbon nanotubes (Wang et al. 2014) have been tested as fillers to improve mechanical behavior of denture materials. Nanoparticles of silica (Da Silva et al. 2012; Balos et al. 2014), silver (Acosta-Torres et al. 2012; Sodagar et al. 2012; de Castro et al. 2016), titanium oxide (Sodagar et al. 2013), as well as ZrO_2 nanotubes (Yu et al. 2014) and a few other nanomaterials (Wilson and Antonucci 2006; Chen 2010; Xu et al. 2017) have also been used to reinforce thermopolymerized acrylic resins. Additives such as silver and zinc oxide, well known for their excellent antibiotic properties, may also reduce inflammation caused by the adhesion of microorganisms (Acosta-Torres et al. 2012; de Castro et al. 2016), further improving the performance of composite resins.

The addition of nanomaterials, nevertheless, not always improves the mechanical properties of the final product (Rawan and AlKahtani 2018). The incorporation of titanium oxide nanoparticles in the thermopolymerized acrylic resins, for example, has been shown to affect adversely the flexural strength of the composite with increasing NP concentration (Nazirkar et al. 2014). In one of the first studies investigating the effect of nanoparticle addition in self-curing acrylic resins, similarly, no major improvement in flexural strength has been observed after the addition of a small proportion (0.05–1%) of Ag, SiO_2, or TiO_2 nanoparticles of approximately 20 nm in diameter (Sodagar et al. 2012; Sodagar et al. 2013). It is interesting to note that in such studies, and in others performed by Balos et al. (2014), Wang et al. (2014), and NazirKar et al. (2014), the best results in flexural strength has occurred when low levels of nanoparticle loads were used, both in self-curing and thermopolymerized acrylic resins.

Surface compatibilization aiming to improved interfacial adhesion and more effective dispersion of the filler into the matrix has been pointed out as a critical step to produce nanocomposite with superior mechanical properties. For example, silanization of silica nanoparticles via the 3-trimethoxysilyl-propyl methacrylate (MPS), coupling agent has been used as a promising method to mix inorganic nanoparticles to resinous matrices (Sideridou and Karabela 2009; Karabela and Sideridou 2011). The silane groups on the surface of the nanoparticles copolymerize with the methacrylic polymer matrix, promoting bonding with the resin and yielding superior performance of the resultant composites (Mohsen and Craig 1995).

In spite of previous efforts, there are still a limited number of studies in the literature on the behavior of self-curing acrylic resins reinforced with nanomaterials. The overall effect of the nanofillers on the mechanical performance of such nanocomposites is controversial and needs further investigation. In the present work, the effect of adding silanized or non-silanized silica nanoparticles of ~ 160 nm in diameter, at different concentrations, on the mechanical properties and surface roughness, a self-cured acrylic resin is reported.

Materials and methods

Materials

All reagents used were of analytical grade from Sigma-Aldrich (ethanol, ammonium hydroxide (30%), tetraethyl orthosilicate (TEOS), 3-trimethoxysilyl-propyl methacrylate (MPS), cyclohexane, n-propylamine). The acrylic resin used is composed by methacrylate and polymethyl methacrylate in a proportion of 3:1 (ISO 20795-1 2013) and was acquired from Jet Artigos Odontológicos Clássico LTDA (Brazil). The hydrocolloid was acquired from Cavex Colorchange.

Synthesis and characterization of silica nanoparticles

The silica nanoparticles (SiO_2-NPs) were prepared following the Stöber process (Stober and Fink 1968). Ultrapure water (6.2 mol), ethanol (1.9 mol), and ammonium hydroxide (0.62 mol) were mixed in round-bottomed flask under magnetic stirring. In a separatory funnel, TEOS (22.4 mmol) and ethanol (0.17 mol) were also mixed and added in the solution. The system was kept under constant magnetic stirring for 4 h at 25 °C. The resultant nanoparticle dispersion was centrifuged (KC5-Kindly) at 3000 rpm for 30 min to allow total decanting of the particles. The supernatant was discarded, and the particles were further washed with ethanol in successive cycles of centrifugation. The

remaining powder of SiO_2 nanoparticles was oven-dried at 120 °C. The SiO_2-NPs were then functionalized with MPS, following the procedure of Karabela and Sideridou (2008). In a round-bottom flask, 1.0 g of SiO_2-NP was mixed with cyclohexane (0.18 mol), n-propylamine (0.34 mmol), and MPS (2.8 mmol) and stirred for 30 min. The mixture was placed in a reflux system at 60 °C for further 30 min, and after that, it was rotary-dried at 60 °C. The remaining solid was oven-dried at 80 °C for 4 h. The final powder of silanized nanoparticles (s-SiO_2-NP) was stored in a desiccator.

The size distribution and the morphology of the dry nanoparticles were obtained from scanning electron microscopy images (SEM-FEG, Inspect-F50 model, FEI). The particle diameter was measured using the ImageJ software, counting at least 100 particles per image. The hydrodynamic diameter of nanoparticles dispersed in water at 25 °C was also obtained by dynamic light scattering (DLS), using a Zetasizer (ZS-ZEN3600, Malvern). The chemical structure was evaluated by infrared spectroscopy (FTIR-Spectrum One, PerkinElmer), using pellets prepared with a mass ratio of 10% of nanoparticles to 90% of KBr. The spectra were obtained in the frequency range of 400–4000 cm^{-1}.

Specimen preparation

Specimens of pure and composite resins were produced following ISO recommendations (ISO 20795-1 2013). A metal mold ($65 \times 40 \times 5$ mm^3) was embedded with hydrocolloid in a dental flask to produce a rectangular volume, where the resins were poured. Two methodologies were employed in the nanocomposite preparation: the NPs were incorporated either in the polymer (powder) or in the monomer (liquid). In order to disperse the nanoparticles in the monomer, the mixture was agitated in an ultrasonic bath for 3 min. In the case of the polymer, the nanoparticles were just mixed manually with the powder. The amount of 1 wt% SiO_2 was added either into the polymer or monomer phase. Considering the manufacturer ratio of polymer/monomer (3:1), the adjusted value of the overall mixture was 0.7 wt% when nanofillers were added into the polymer, and 0.27 wt% when inserted into the monomer phase. The low amount of silica nanoparticles used in this study was chosen due to indications in previous works that low content of nanofillers yield the most favorable results (Balos et al. 2014; Wang et al. 2014; Cevik and Bicer 2016).

The mixtures with nanoparticles were placed into the rectangular mold in the dental flask and pressed to 1 t. In the self-curing process, solidification is quick (~ 4 min), and the process is completed within ~ 15 min. After curing, each sample was cut longitudinally in a milling machine (Clever) in three equal stripes (64 mm long, 10.0 ± 0.2 mm wide, and 3.3 ± 0.2 mm thick). The as-prepared specimens were stored in distilled water at 37 °C, for 50 ± 2 h (ISO 20795-1 2013; Sodagar et al. 2013; Nazirkar et al. 2014).

Group division

Five groups (with $n = 6$) were created: the control (pure resin) plus 4 test groups (G1 to G4), where NPs were added (Table 1). They differ in nanofiller content and method of NP incorporation. In the group G1, SiO_2-NPs were added into the polymer powder, totaling 0.7 wt% of the overall mixture. In the group G2, SiO_2-NPs were added to the liquid monomer, making 0.27 wt% of the overall mixture. In the group G3, a total of 0.7 wt% of silanized nanoparticles (s-SiO_2-NP) was incorporated into the polymer. In the group G4, 0.27 wt% of s-SiO_2-NP was added to the monomer. For each group, measurements of the flexural strength, surface roughness, and Vickers microhardness were performed, as described below.

Surface roughness test

Five samples per group ($n = 5$) were polished in a Struers polishing machine (DPU-10, Panambra, Brazil), under constant refrigeration, using metallographic sandpapers in a sequence (P500, P1000, P1200) recommended by ISO ("ISO 20795-1" 2013). The surface roughness (Ra, arithmetical mean height) of each specimen was measured using a digital profilometer (SJ 201 Mitutoyo, Japan), attached to a metal base to eliminate unwanted vibrations and assure reading fidelity. The profiler moved the diamond stylus across 0.25 mm of the sample under a constant load. Three readings per specimen were performed.

Nanoscale roughness was also recorded in selected samples with a scanning force microscope (Icon, Bruker). As-polished surfaces and microtomed facets from cross-sectioned specimens were imaged, using the peak force tapping mode and TESP 150 or ScanAssist Air Si tips. The imaged area for local nanoscale roughness analysis was 1×1 μm^2, but images

with scanning lateral sizes of up to 40 μm were collected for global topography evaluation.

Flexural strength test

The stripes for the flexural strength test (64 mm × 10 mm × 3.3 mm) were prepared following ISO 20795-1:2013. Samples were tested until fracture in a universal testing machine (EMIC DL—2000) at a cross-head speed of 5 mm/min and using a 50 kgf load cell. The ultimate strength of the specimens were recorded.

Microhardness test

Two samples per group were submitted to Vickers microhardness test in a Fischerscope H100 equipment, according to ISO-14577. Prior to the measurements, the sample surfaces were examined through a microscope (magnification × 10) in order to search for zones free of bubbles or flaws. Ten indentations were performed in flawless areas of each sample with a Berkovich pyramid diamond penetrator, with a maximum load of 200 mN in a charge-discharge cycle of 80s.

Statistical analysis

Data were firstly submitted to Shapiro-Wilk normality test and then evaluated by one-way ANOVA, followed by post hoc Tukey test, when significant differences between groups were found. The significance level was considered $p < 0.05$. Data were analyzed by the GraphPad Prism software and presented as mean values ± the standard deviation.

Table 1 Description of test groups according to the type, concentration, and incorporation method of the nanoparticles in the acrylic resins

Groups	wt%	Incorporation	Nanoparticles
Ctrl ($n = 6$)	–	–	–
G1 ($n = 6$)	0.70	polymer	SiO_2-NP
G2 ($n = 6$)	0.27	monomer	SiO_2-NP
G3 ($n = 6$)	0.70	polymer	s-SiO_2-NP
G4 ($n = 6$)	0.27	monomer	s-SiO_2-NP

Results and discussion

Characteristics of the synthesized nanoparticles

Figure 1 depicts the major physicochemical characteristics of the as-prepared nanoparticles. Scanning electron microscopy (SEM) images of pristine and silanized SiO_2 nanoparticles are shown in Fig. 1a–b, respectively, revealing particles of spherical geometry similar to what is found in commercial formulations. The respective size distributions are given in the insets of Fig. 1a–b. No significant differences in size or geometry were observed between silanized and non-silanized nanoparticles. The mean diameters obtained from such distributions were 169 ± 32 nm for SiO_2-NP and 142 ± 60 nm for s-SiO_2-NP. The larger size dispersion in s-SiO_2-NP stems from the bimodal character of the distribution, with peaks at ~ 70 nm and ~ 180 nm. The size distribution of the nanoparticles in aqueous solution was also measured by DLS and is presented in Fig. 1c. The mean values obtained from such distributions were 164 nm for SiO_2-NP and 209 nm for s-SiO_2-NP. Hydrodynamic and dried nanoparticle diameters were similar, but for silanized nanoparticles, a more pronounce tail toward larger particle sizes was seen. The enhancement of the hydrodynamic radius for s-SiO_2-NP can be attributed to the functionalization of the silica surface via the incorporation of methacrylate groups.

The absorption spectra of the nanoparticles in the infrared region are shown in Fig. 1d. The spectrum of the bare silica is dominated by the absorption band around 1098 cm^{-1} characteristic of the stretching of Si–O–Si bonds. This band is shifted to lower wavenumbers in the silanized nanoparticles. Other bands include the stretching of hydroxyl groups terminating the surface of the silica nanoparticles (Si–OH bonds) at 921 cm^{-1} and the absorption band at 788 cm^{-1} assign also to Si–O–Si bonds. The weak bands seen in the region of 1724 cm^{-1} are stretching vibration from carbonyl groups (C=O) and at 1461 cm^{-1} are from C=C of methacrylate group, which are present in the s-SiO_2-NP samples (Karabela and Sideridou 2008).

Microstructure and roughness of the nanocomposite resins

Figure 2 shows electron microscopy images of as-polished pristine and nanoparticle-loaded resins. A relatively smooth surface is observed for the control sample

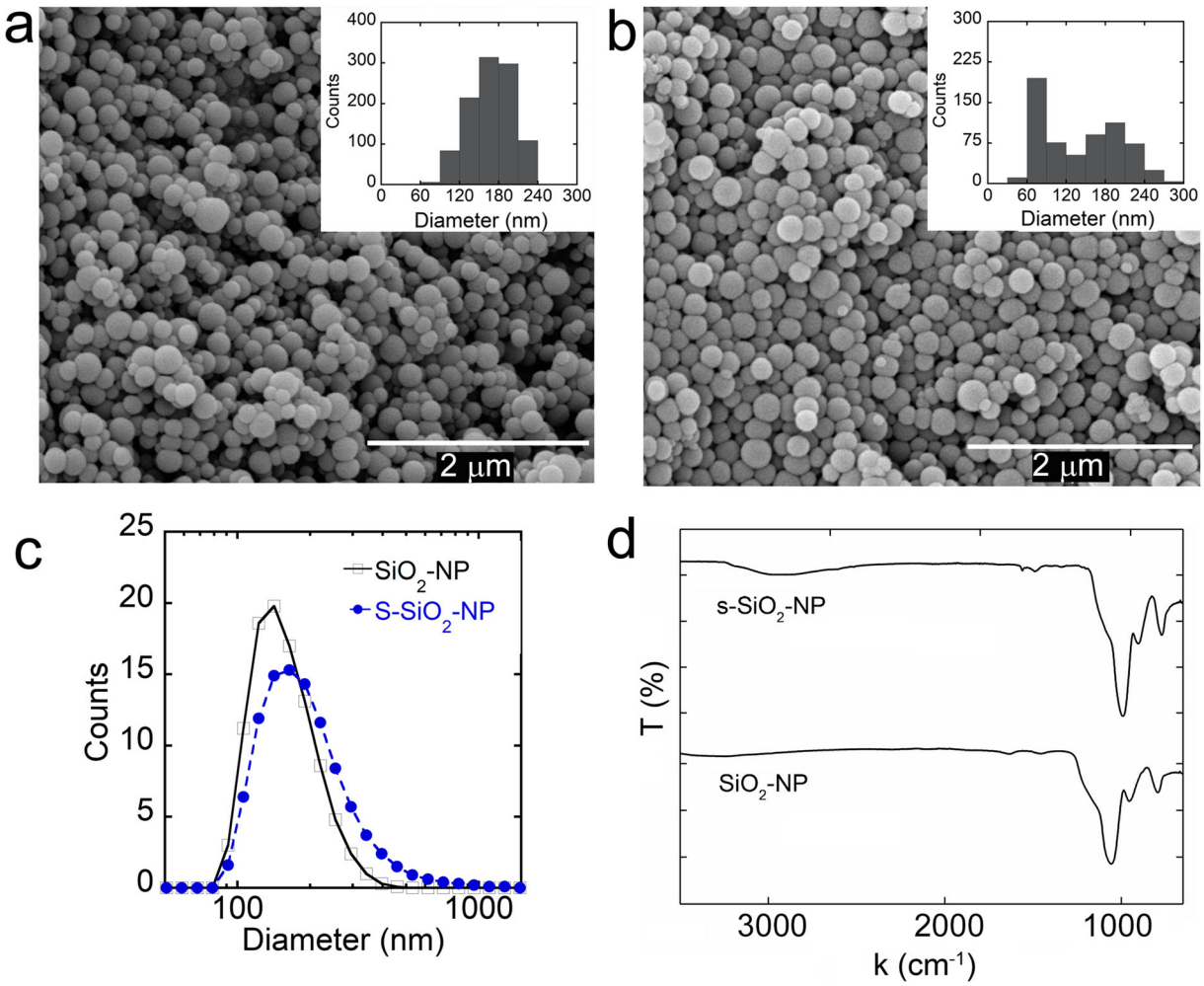

Fig. 1 Scanning electron microscopy images and respective histograms of the size distribution of silica nanoparticles: **a** SiO_2-NP and **b** s-SiO_2-NP. **c** Size distribution by DLS of silica nanoparticles (SiO_2-NP (-) and silanized nanoparticles s-SiO_2-NP (●) in aqueous solution. **d** FTIR spectra of silanized and non-silanized silica nanoparticles

(Fig. 2a). Images from G1 samples are also dominated by similar smooth areas, but in certain places, large inclusions characterized by a brighter contrast and a rougher topology are also seen (Fig. 2b). A zoom on those regions (Fig. 2c) reveals the presence of clusters of spherical particles with sizes compatible with the SiO_2-NPs. Energy dispersive X-ray analysis (EDS) confirms the presence of a large fraction of Si (~ 30%) at such areas. Thus the whitish areas on the images are large agglomerates of SiO_2 nanoparticles (which can be over 50 μm across). For the G2 samples, the microstructure was similar to the G1 group, but agglomerates are less frequent, as expected. Samples from groups G3 to G4 made with silanized NPs show a distinct structure. The presence of the large clusters was further diminished in G3 samples. The aggregates in G3 showed a reduced content of Si as compared to those in samples from groups G1 or G2, indicating a larger separation between nanoparticles. For the G4 group, no large agglomerates were observed during SEM analysis, and the EDS spectra taken in various spots did not detect the presence of Si.

The mean surface roughness R_a obtained from profilometry of samples prepared from pure and reinforced resins are presented in Fig. 3 and Table 2. R_a varies between groups, ranging from 0.17 (in the control group) up to 0.31 μm (in group G2 where 0.27 wt% of SiO_2-NP was incorporated into the monomer). Although the values of the surface roughness found for all nanoparticle-loaded groups increased when compared to the control group, the detected changes were not statistically significant ($p = 0.21$). Resins prepared

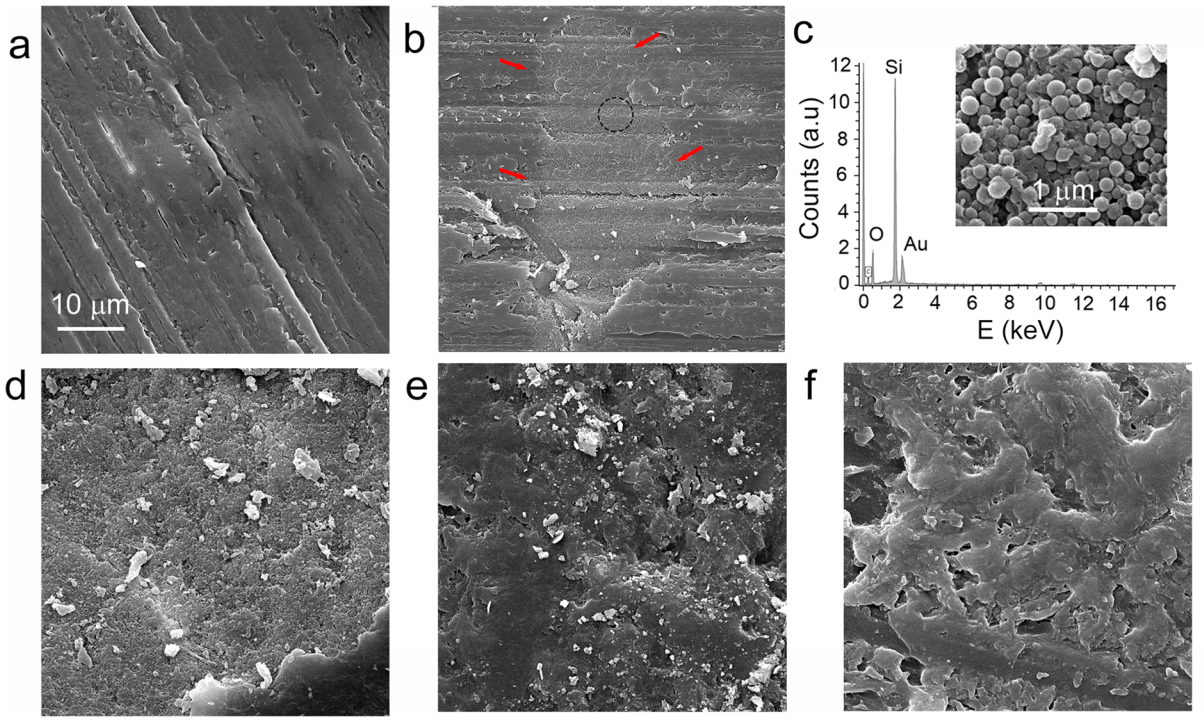

Fig. 2 Scanning electron microscopy (SEM) micrographs of control and nanocomposite samples of the study groups. All images were collected with equal magnification, and the scale bar in **a** applies to all frames, except **c** which shows a zoomed region. **a** As-polished specimen of unmodified self-cured resin. **b** Sample from group G1 (SiO_2-NP incorporated in the polymer), showing a region with a large aggregate marked by the arrows. **c** Zoom over the region in **b** identified by the dashed circle and respective EDS spectrum. **d** Sample from group G2 (SiO_2-NP incorporated in the monomer). **e** Sample from group G3 (s-SiO_2-NP incorporated in the polymer). **f** Sample from group G4 (s-SiO_2-NP incorporated in the monomer)

with silanized nanoparticles presented the lowest surface roughness, close to the pristine resin, this being possibly a favorable aspect for achieving topographical uniformity in the acrylic samples.

AFM images shown in Fig. 4 allow a more detailed investigation of subtle changes in the local nanoscale roughness between pure and nanoparticle-loaded resins of G4 (0.27% of silica loaded in the liquid). The pure resin has a local R_a (at a length scale of 1 μm) of 5.9 nm, while for the nanocomposite protruding spherical features (comparable to the dimensions of buried nanoparticles) appear more often on the surface and $R_a = 9.2$ nm. This difference in R_a arises basically from the increased

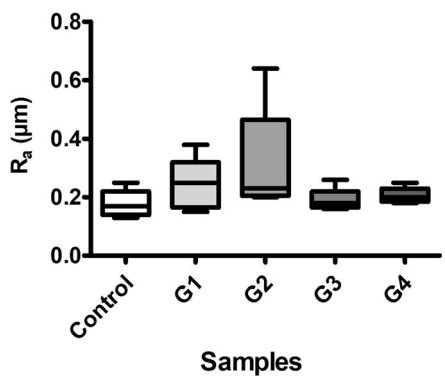

Fig. 3 Surface roughness (R_a) from control, G1, G2, G3, and G4 samples. ($n = 6$; mean ± SD; ANOVA followed by Turkey post-hoc)

Table 2 Flexural strength, microhardness, and roughness mean values and standard deviations for all experimental groups

Group	Flexural strength (σ) (MPa)	Hardness (VHN) (kg/mm^2)	Roughness (R_a) (μm)
Ctrl	82.0 ± 2.4^a	22.8 ± 2.6^a	0.17 ± 0.04^a
G1	61.5 ± 8.5^{ab}	22.5 ± 2.1^a	0.24 ± 0.08^a
G2	66.7 ± 6.3^{ab}	21.6 ± 2.1^a	0.31 ± 0.18^a
G3	67.2 ± 9.8^{ab}	22.6 ± 1.3^a	0.19 ± 0.04^a
G4	59.9 ± 21.4^b	23.1 ± 4.0^a	0.20 ± 0.02^a

Averages in columns are followed by the letter *a* when they are not stattistically different from the control and *b* when the difference is statistically significant

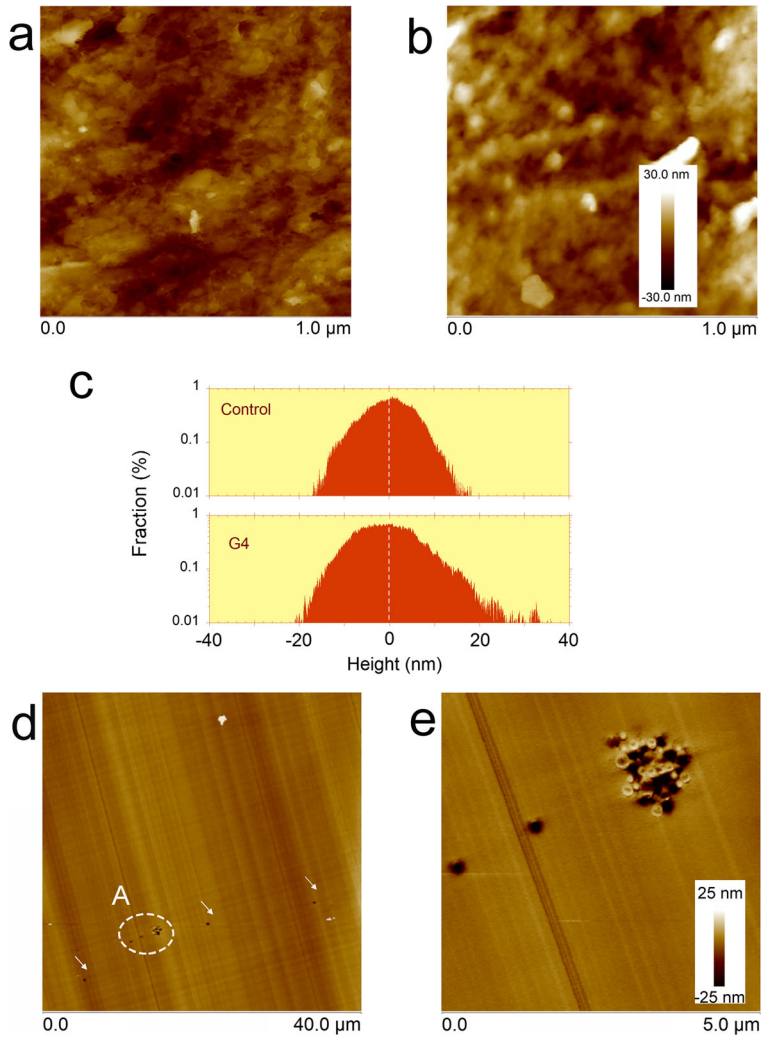

Fig. 4 AFM images of **a** pure and composite **b** resin loaded with 0.27% in the liquid (G4), showing local nanoscale roughness across a lateral scan of 1 μm. The color scale in **b** applies for both images. **c** Height frequency histograms from images **a** and **b**. **d**–**e** AFM images of the interior of a G4 resin, obtained from cross sections of the specimen. The height color scale is the same for both images. **d** Small dark points indicated by the arrows are voids from sites where presumably nanoparticles were present. The ellipse *A* highlight an agglomerate. **e** Zoom around the region *A* in **b**, allowing a closer view of the agglomerate and two individual cavities. Note that the bright circular spots appearing in the cluster are concave, like bowls. Both the dark voids and the bright concave spots are interpreted as sites where nanoparticles were located before the sectioning of the sample

frequency of surface heights between + 10 and 30 nm, as can be seen from the histogram of the images in Fig. 4c. Naturally, the local roughness varies depending on the probed lateral size, but for AFM images with scanning sizes of about 40 μm, the values of R_a obtained by profilometry and AFM are comparable.

In order to obtain information of the interior parts of the resins, specimens were cut in cross section, and a smooth surface was prepared on the block by means of a microtome knife. AFM images of such cross-sectioned parts on a specimen from G4 (where large aggregates were not seen in the SEM images) are shown in Fig. 4d–e. Large areas of uniform surface topography are combined with regions where circular voids and concave protruding regions (in the form of a bowl) are seen. Such structures have lateral sizes comparable with the dimensions of single nanoparticles (100–200 nm). An agglomerate of a size approximately 1000 nm is also clearly visible in the image. Even larger agglomerates 2–5 μm across were observed in other images. These structures indicate, most probably, sites where silica nanoparticles were initially present but were removed by the microtome blade in the sectioning processes. For the other test groups, equivalent structures were seen in the AFM images, always appearing as 100–200-nm size voids or concave protrusions, but organized in much larger (and rare) clusters. Thus, both SEM analysis and the high-resolution AFM images suggest that silanization results in better nanoparticle dispersion. The fact that R_a obtained from submillimeter scans of a profilometer is smaller in silanized groups is also an indication of better dispersibility in silanized resins.

Mechanical behavior of the nanocomposite resins

The results for the mechanical tests of microhardness (VHN) and flexural strength (σ) are shown in Figs. 5 and 6. The respective average, standard deviation, and Tukey analysis outcomes are presented in Table 2. The microhardness values of nanocomposite resins are only slightly different from the pure resin (less than 5%, and changes are not statistically significant $p = 0.79$). Although we could not find data on self-cured resins in the literature to compare with, results from thermopolymerized resins filled with nanosilica are contradictory in this respect. For example, Cevik and Bicer similarly have not found significant differences in the hardness of thermopolimerized resins after addition of 1% or 5% silica (Cevik and Bicer 2016). On the other hand, in a study where low silicate loadings were used (from 0.023 to 0.91% by volume), most of the specimens showed increased microhardness ($p < 0.01$), especially those with the smallest content of nanosilica (Balos et al. 2014). Finally, in another study where silanized silica nanoparticles were incorporated into microwave-polymerized resins (at concentrations between 0.1 and 5.0%), statistically significant reductions in the hardness of the nanocomposite resins were observed in comparison with the pristine formulation. The decrease was larger the greater the filler content, reaching about 38% at the highest nanoparticle concentration (Da Silva et al. 2012). Thus, considering such conflicting results, it appears that the effective hardness of the composite material is very sensitive to the processing method. It may also be strongly influenced by inhomogeneities in composition introduced by the

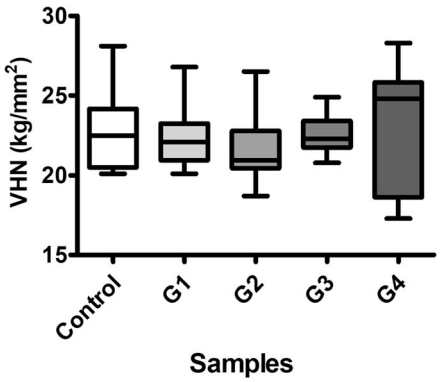

Fig. 5 Box plot of microhardness (VHN) measurements obtained from control, G1, G2, G3, and G4 samples. ($n = 6$; mean ± SD; ANOVA followed by Turkey post hoc)

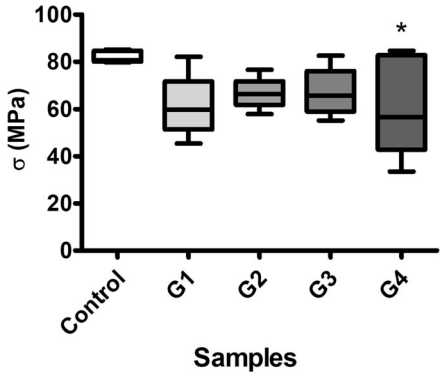

Fig. 6 Box plot of the flexural strength (σ) obtained from control, G1, G2, G3, and G4 samples. Significant differences compared to the control were observed only for the G4 group

aggregation of the nanofiller, what seems to be a common feature in dental nanocomposite resins reported in the literature, although direct evidence of the nanoparticle distribution is not always provided in such works.

The mean flexural strength of the composite resins varied from 59.9 (G4) to 67.2 MPa (G3) and were always smaller than in the pure resin (82.0 MPa), as can be seen in Fig. 6. The differences were found statistically significant only for the G4 group ($p = 0.0534$), when 0.27 wt% of s-SiO_2-NP were incorporated in the monomer. The flexural strength of the G4 group reached the lower limit of resin performance proposed by the ISO ($\sigma > 60$ MPa (ISO 20795-1 2013). Thus, addition of either silanized or non-silanized silica nanoparticles at the employed concentrations did not change significantly hardness but may adversely affect the flexural strength of the self-cured resins. Sodagar et al. (2013) have also found substantially reduced flexural strength values with the addition of 0.5% and 1% of non-silanized SiO_2-NP (~ 20 nm) into the monomer of a self-cured acrylic resin, although their control values (~ 43 MPa) were much smaller than the ones reported here. These and other authors have found that the composite with the largest content of nanoparticles had the largest decrease in σ (Sodagar et al. 2013; Balos et al. 2014; Cevik and Bicer 2016), a trend not seen in our samples.

Insufficient dispersion and aggregation of the filler in the acrylic matrix has been raised as a possible cause of the adverse effect of silica on flexural strength in Sodagar's work (Sodagar et al. 2013), what might also apply to our results. Agglomerated fillers interposed between polymeric chains may reduce the interlocking of fibers and act as a stress-concentrating agent in the acrylic resin, compromising flexural performance. Agglomeration was directly probed in our tested groups by

atomic force and electron microcopy as discussed in the previous section, and two classes of clusters were found: large agglomerates extending for several tens of micrometers (mostly found in non-silanized silica composites) and small clusters seen by AFM in the silanized silica group G4. In an attempt to mitigate particle agglomeration and following the methodology described by Balos et al. (2014), the use of a probe ultrasound sonicator (instead of the low-intensity ultrasonic bath) was also tested to assist the dispersion of the NPs in the monomer. Due to the high-power of the probe sonicator, the monomer/nanoparticle mixture was kept in an ice bath to avoid excessive heating. Still, samples prepared in this way showed no clear improvement in terms of nanoparticle dispersion. The short time available in the self-curing process for the mixture to homogenize (before mobility is frozen) poses additional challenges to achieve high filler dispersion in this class of resins (as compared to the thermopolymerized ones). Indeed, preventing agglomeration has been one of the main challenges in the production of high-quality nanocomposites (Sideridou and Karabela 2009; Sodagar et al. 2013; Nazirkar et al. 2014; Wang et al. 2014; Cevik and Bicer 2016).

It is important to note that even the use of silanized particles, which in principle could provide a better interfacial connection between the inorganic and organic phases and thus improve dispersibility of the particles (Karacaer et al. 2003; Sideridou and Karabela 2009; Karabela and Sideridou 2011), did not enhanced substantially the properties of the material. The overall performance of the composites based on silanized nanoparticles was nevertheless slightly better. Among all test groups, G3 and G4 showed the highest levels of hardness and the smallest increase in surface roughness compared to the pure resin. Additional studies are required using other NPs sizes, different types of silanes, and exploring alternative methods of nanoparticle dispersion in order to address the issue of the nanofiller dispersion and to achieve the desired goal of larger flexural strength in nanocomposite self-cured resins.

Conclusion

Incorporation of silanized and non-silanized silica nanoparticles into self-curing acrylic resins affected mechanical properties and surface roughness of the dental material. Nanoparticle-loaded resins presented similar microhardness to the pristine formulation for all conditions tested. Nevertheless, nanocomposite resins showed an unwanted reduced flexural strength (20–27%) which was neither dependent on the amount of filler added nor in the method of nanoparticle incorporation. Surface silanization, usually considered beneficial for matrix-filler bonding, caused no major improvement in the mechanical behavior of the nanoresins. Yet, silanization appears to improve nanoparticle dispersibility as indicated by the reduction in the size of aggregates and by the smaller surface roughness observed in these groups. Achieving good nanoparticle dispersion (during the short time available before molecular mobility is frozen in the curing process) appears to be the main challenge in the production of self-cured nanocomposite resins with improved flexural strength.

Funding This work was financed by the Brazilian agencies CAPES (finance code 001) and by the National Institute of Science and Technology of Surface Engineering (INCT-INES-contract 465423/2014-0, CNPq).

Compliance with ethical standards The study was approved at the Local Ethical Committee of School of Heath Sciences of Pontifical Catholic University of Rio Grande do Sul (Application #9216).

Conflict of interest The authors declare that they have no conflict of interest.

References

Acosta-Torres LS, Mendieta I, Nuñez-Anita RE, Cajero-Juárez M, Castaño VM (2012) Cytocompatible antifungal acrylic resin containing silver nanoparticles for dentures. Int J Nanomed 7: 4777–4786. https://doi.org/10.2147/IJN.S32391

Balos S, Pilic B, Markovic D, Pavlicevic J, Luzanin O (2014) Poly(methyl-methacrylate) nanocomposites with low silica addition. J Prosthet Dent 111(4):327–334. https://doi.org/10.1016/j.prosdent.2013.06.021

Bertassoni LE, Marshall GW, de Souza EM, Rached RN (2008) 'Effect of pre- and postpolymerization on flexural strength and elastic modulus of impregnated, fiber-reinforced denture base acrylic resins. J Prosthet Dent 100(6):449–457. https://doi.org/10.1016/S0022-3913(08)60263-2

Bollen CM, Lambrechts P, Quirynen M (1997) 'Comparison of surface roughness of oral hard materials to the threshold surface roughness for bacterial plaque retention: a review of the literature. Dent Mater 13(4):258–269. https://doi.org/10.1016/s0109-5641(97)80038-3

Borchers L, Tavassol F, Tscernitschek, h. (1999) Surface quality achieved by polishing and by varnishing of temporary crown

and fixed partial denture resins. J Prosthet Dent 82(5):550–556 https://doi-org.ez94.periodicos.capes.gov.br/10.1016/S0022-3913(99)70053-3

Cevik P, Bicer A (2016) The effect of silica and prepolymer nanoparticles on the mechanical properties of denture base acrylic resin. J Prosthodont 00:1–8. https://doi.org/10.1111/jopr.12573

Chen MH (2010) Update on dental nanocomposites. J Dent Res 89(6):549–560. https://doi.org/10.1177/0022034510363765

Da Silva L, Feitosa S, Valera M, De Araujo M, Tango R (2012) Effect of the addition of silanated silica on the mechanical properties of microwave heat-cured acrylic resin. Gerontology 29:1019–1023. https://doi.org/10.1111/j.1741-2358.2011.00604.x

de Castro DT, Valente ML, da Silva CH, Watanabe E, Siqueira RL, Schiavon MA, Alves OL, Dos Reis AC (2016) 'Evaluation of antibiofilm and mechanical properties of new nanocomposites based on acrylic resins and silver vanadate nanoparticles. Arch Oral Biol 67:46–53. https://doi.org/10.1016/j.archoralbio.2016.03.002

Franklin P, Wood DJ, Bubb NL (2005) 'Reinforcement of poly(methyl methacrylate) denture base with glass flake. Dent Mater 21(4):365–370. https://doi.org/10.1016/j.dental.2004.07.002

'ISO 20795-1 Dentistry,Base polymers, Part 1: Denture base polymers', (2013). http://primo-pmtna01.hosted.exlibrisgroup.com/PUC01:PUC01:puc01000489268

Kanie T, Arikawa H, Fujii K, Ban S (2004) 'Flexural properties of denture base polymers reinforced with a glass cloth-urethane polymer composite. Dent Mater 20(8):709–716. https://doi.org/10.1016/j.dental.2003.11.007

Karabela MM, Sideridou ID (2008) Effect of the structure of silane coupling agent on sorption characteristics of solvents by dental resin-nanocomposites. Dent Mater 24(12):1631–1639. https://doi.org/10.1016/j.dental.2008.02.021

Karabela MM, Sideridou ID (2011) Synthesis and study of properties of dental resin composites with different nanosilica particles size. Dent Mater 27(8):825–835. https://doi.org/10.1016/j.dental.2011.04.008

Karacaer O, Polat TN, Tezvergil A, Lassila LV, Vallittu PK (2003) 'The effect of length and concentration of glass fibers on the mechanical properties of an injection- and a compression-molded denture base polymer. J Prosthet Dent 90(4):385–393. https://doi.org/10.1016/S0022391303005183

Kim SH, Watts DC (2004a) 'Exotherm behavior of the polymer-based provisional crown and fixed partial denture materials. Dent Mater 20(4):383–387. https://doi.org/10.1016/j.dental.2003.11.001

Kim SH, Watts DC (2004b) 'The effect of reinforcement with woven E-glass fibers on the impact strength of complete dentures fabricated with high-impact acrylic resin. J Prosthet Dent 91(3):274–280. https://doi.org/10.1016/S0022391303008679

Mohsen NM, Craig RG (1995) Effect of silanation of fillers on their dispersability by monomer systems. J Oral Rehabil 22:183–189. https://doi.org/10.1111/j.1365-2842.1995.tb01562.x

Nazirkar G, Bhanushali S, Singh S, Pattanaik B, Raj N (2014) 'Effect of anatase titanium dioxide nanoparticles on the flexural strength of heat cured poly methyl methacrylate resins: an in-vitro study. J Indian Prosthodont Soc 14(Suppl 1):144–149. https://doi.org/10.1007/s13191-014-0385-8

Rawan N, AlKahtani (2018) The implications and applications of nanotechnology in dentistry: a review. Saudi Dent J 30:107–116

Sideridou ID, Karabela MM (2009) Effect of the amount of 3-methacyloxypropyltrimethoxysilane coupling agent on physical properties of dental resin nanocomposites. Dent Mater 25(11):1315–1324. https://doi.org/10.1016/j.dental.2009.03.016

Sodagar A, Kassaee M, Akhavan A, Javadi N, Arab S, Kharazifard M (2012) Effect of silver nano particles on flexural strength of acrylic resins. J Prosthodont Res 56:120–124 https://doi-org.ez94.periodicos.capes.gov.br/10.1016/j.jpor.2011.06.002

Sodagar A, Bahador A, Khalil S, Shahroudi A, Kassaee M (2013) The effect of TiO2 and SiO2 nanoparticles on flexural strength of poly (methyl methacrylate) acrylic resins. J Prosthod Res 57:15–19 https://doi-org.ez94.periodicos.capes.gov.br/10.1016/j.jpor.2012.05.001

Stober W, Fink A (1968) Controlled growth of monodisperse silica spheres in the micron size range. J Colloid Inertface Sci 26:62–68 https://doi-org.ez94.periodicos.capes.gov.br/10.1016/0021-9797(68)90272-5

Straioto FG, Ricomini Filho AP, Fernandes Neto AJ, Del Bel Cury AA (2010) Polytetrafluorethylene added to acrylic resins: mechanical properties. Braz Dent J 21(1):55–59. https://doi.org/10.1590/S0103-64402010000100009

Wang R, Tao J, Yu B, Dai L (2014) 'Characterization of multiwalled carbon nanotube-polymethyl methacrylate composite resins as denture base materials. J Prosthet Dent 111(4):318–326. https://doi.org/10.1016/j.prosdent.2013.07.017

Wilson KS, Antonucci JM (2006) Interphase structure-property relationships in thermoset dimethacrylate nanocomposites. Dent Mater 22(11):995–1001. https://doi.org/10.1016/j.dental.2005.11.022

Xu X, He L, Zhu B, Li J, Li J (2017) Advances in polymeric materials for dental applications. Polym Chem 8:807–823. https://doi.org/10.1039/C6PY01957A

Yamauchi M, Yamamoto K, Wakabayashi M, Kawano J (1990) 'In vitro adherence of microorganisms to denture base resin with different surface texture. Dent Mater J 9(1):19–24. https://doi.org/10.4012/dmj.9.19

Yu W, Wang X, Tang Q, Guo M, Zhao J (2014) Reinforcement of denture base PMMA with ZrO(2) nanotubes. J Mech Behav Biomed Mater 32:192–197. https://doi.org/10.1016/j.jmbbm.2014.01.003